Atmospheric Environment 96 (2014) 163–174

Contents lists available at ScienceDirect

Atmospheric Environment

journal homepage: www.elsevier.com/locate/atmosenv

Magnetic evaluation of TSP-filters for air quality monitoring

Ana Gabriela Castañeda-Miranda [a, *], Harald N. Böhnel [b], Roberto S. Molina-Garza [b], Marcos A.E. Chaparro [c]

[a] Posgrado en Ciencias de la Tierra, Universidad Nacional Autónoma de México, Blvd. Juriquilla 3001, Querétaro 76230, Mexico
[b] Centro de Geociencias, Universidad Nacional Autónoma de México, Blvd. Juriquilla 3001, Querétaro 76230, Mexico
[c] Centro de Investigaciones en Física e Ingeniería del Centro de la Provincia de Buenos Aires (CIFICEN, CONICET-UNCPBA), Pinto 399, 7000 Tandil, Argentina

HIGHLIGHTS

- We studied magnetic properties and SEM particle analysis in hi-vol air samplers.
- TSP determined by conventional methods correlates well with magnetic susceptibility.
- The magnetic signal is mostly derived from PSD magnetite particles.
- Measurements suggest that susceptibility is a fast, low-cost, proxy for TSP monitoring.

ARTICLE INFO

Article history:
Received 13 August 2013
Received in revised form
2 July 2014
Accepted 3 July 2014
Available online 7 July 2014

Keywords:
Environmental monitoring
Magnetic properties
Atmospheric pollution
Heavy metals
Anthropogenic airborne particles

ABSTRACT

We present the magnetic properties of the powders collected by high volume total suspended particle air samplers used to monitor atmospheric pollution in Santiago de Querétaro, a city of one million people in central Mexico. The magnetic measurements have been combined with scanning electron microscopy observations and analysis, in order to characterize the particles captured in the filters as natural and anthropogenic. The main goal of the study is to test if magnetic measurements on the sampled atmospheric dust can be effective, low-cost, proxy to qualitatively estimate the air quality, complementing the traditional analytical methods. The magnetic properties of the powder collected in the filters have been investigated measuring the low field magnetic susceptibility, hysteresis loops, thermomagnetic curves, and isothermal remanent magnetization. The rock magnetism data have been supplemented by energy-dispersive X-ray spectroscopy analysis and Raman spectroscopy. It was found that the main magnetic carrier is low-Ti magnetite in the PSD range with a contribution from SP particles, and small but significant contributions from hematite, maghemite and goethite particles. Total suspended particles in the atmosphere during the monitored days ranged between about 30 and 280 $\mu g/m^3$. Magnetic susceptibility values are well correlated with the independently determined total suspended particles concentration ($R = 0.93$), but particle concentration does not correlate as well with IRM1T. This may be attributed to contributions from SP and paramagnetic particles to the susceptibility signal, but not to the remanence. The effects of climate in particle size, composition and concentration were considered in terms of precipitation and wind intensity, but they are actually minor. The main effect of climate appears to be the removal of SP particles during rainy days. There is a contribution to air pollution from natural mineral sources, which we attribute to low vegetation cover in the region's arid climate. The concentration of the magnetic particles and their grain-size vary according to the location of the monitoring station, with higher contributions to anthropogenic Fe-rich particles from vehicle emissions in the city center and other metals in the industrial parks. Metals of interest, usually diagnostic of atmospheric pollution (Fe, As, Sb, Cr, Mo, V, Zn, Ba, Pb, and Cu) were identified by means of electron microscopy.

1. Introduction

Air pollution by airborne particle matter (PM) is a growing problem in urban areas. The activities that produce PM can be broadly divided into industrial and vehicular, which generally take

* Corresponding author.
E-mail address: agmiranda@geociencias.unam.mx (A.G. Castañeda-Miranda).

http://dx.doi.org/10.1016/j.atmosenv.2014.07.015
1352-2310/

place in different areas of the cities. Such activities in areas with rapid growth and urbanization rates have caused an increment in health problems, some of which have been associated with anthropogenic heavy metal particles (Voutsa and Samara, 2002).

Traditionally, the assessment of suspended PM in the atmosphere is carried out using analytical chemical techniques; this implies relatively high operational and instrumentation costs. It is from this perspective that the need to implement rapid and low-cost methods for air quality monitoring arose. Low-cost and speed are some of the attributes of the environmental magnetism methods. These techniques require relatively low budgets, and they are sufficiently sensitive as proxies of a variety of environmental variables and processes (Evans and Heller, 2003).

Environmental magnetism methods have been previously applied to monitor air pollution. Earlier work applied environmental magnetism to dust collected by filters (Muxworthy et al., 2001; Xie et al., 2001; Shu et al., 2001; Sagnotti et al., 2006), and later it took advantage of biological materials such as tree leaves and lichens as biomonitors (e.g., Moreno et al., 2003; Böhm et al., 1998). Research on the magnetic characterization of air filters is important because it allows the comparison of magnetic proxies with conventional monitoring methods, and may validate the application of magnetic techniques in other passive collectors such as tree leaves.

Previous magnetic studies of filters have been carried out in mid-latitude regions with relatively humid temperate climates. Shu et al. (2001) studied the correlation between total suspended atmospheric particles and some magnetic parameters in the Shanghai megalopolis. Applicability of their study on other regions may be, however, limited because of several singularities. Shanghai is a highly industrialized region, and the city size itself makes it a special case. Shu et al. (2001) report that low and high coercivity phases appear in similar proportion in atmospheric dust samples, also with a high contribution of superparamagnetic (SP) particles near a steel-manufacturing complex.

Sagnotti et al. (2006) reported for the first time an empirical linear relationship between magnetic susceptibility and particle matter <10 μm (PM10) concentration. These authors also report a significant difference between fall–winter and spring–summer months in the linear dependence of magnetic susceptibility with PM10. An important contribution of their work is a method for estimating the percentage of non-magnetic material derived from far-sided sources.

Muxworthy et al. (2001) compared magnetic remanence measurements of atmospheric dust with pollution and meteorological data. The dust was collected at monitoring stations in the German city of Munich. The variation in concentration-dependent magnetic parameters was found to be strongly affected by meteorological conditions, whereas composition and grain-size dependent parameters show weak correlation with pollution data. These authors suggest that the magnetic signature may be influenced by dispersion rates of pollutants.

The results from studies in mid-latitude humid temperate sites cannot be blindly extrapolated to the Mexico's highlands because most of the country lies in arid to semi-desert steppe climate belts with low vegetation cover, strong seasonality of humidity and precipitation, and relatively mild winters. Querétaro, our case of study in the Mexican highlands, and typical for most of central Mexico, is also affected by seasonally strong winds and a long (up to 8 months) dry season.

Here we present the results of the magnetic characterization of particles collected in fiberglass filters of Hi-Vol monitoring systems (high volume active air samplers) distributed in the urban area of Santiago de Querétaro, Mexico. The combined magnetic and analytical data can be useful to test if the magnetic susceptibility can be correlated to the TSP, and can be used as a proxy for airborne heavy metal particles and atmospheric pollution in general.

2. Methodology and sampling

2.1. Study area

The city of Santiago de Querétaro, or Querétaro for short, is located in the central Mexico volcanic highlands (20° 36′ N; 100° 24′ W) at about 1820 masl. The metropolitan area occupies about 741 km^2. The city itself is host to about 800 thousand inhabitants, but neighboring municipalities raise the population of the urban area to approximately one million.

Based on limited data, the main cause of air pollution in Querétaro has been attributed to vehicles; it was estimated that about 75% of the contamination is derived from vehicular sources (INEGI, 2003). Gasca (2007) suggested, however, that the main source of airborne particles in the city might be the local industry. In Querétaro mobile sources of pollution have increased significantly over the last decades. Registered vehicles in 2010 reached 195,000 growing at a yearly rate of about 8% (INEGI, 2010).

Vehicles in transit are an important source of pollution. The city is located at the intersection of two of the most important routes in Mexico. Highway 57 accommodates most of the north–south traffic between Mexico City and the US border, including also the city of Monterrey. Highway 35D drives traffic in an east–west direction between Mexico City, the Bajío region and the Pacific coast. The city is also host to five large industrial parks (Fig. 1). Most of the industry is manufacture. In order of volume the most important industries are automobile-parts, appliances, food and beverages, construction, and aerospace.

The city is in the eastern extreme of the Bajío, an E–W trending tectonic depression along the volcanic highlands that hosts the Lerma river system. Local bedrock consists primarily of volcanic and volcaniclastic rocks. The city is surrounded by large volcanic edifices with rocks of intermediate to mafic composition. Cimatario extinct shield volcano is the nearest volcanic structure forming minor highlands. Fault scarps south and east of the city are the most prominent geologic features and are visible in Fig. 1. The Bajío depression is mostly filled by volcaniclastic materials, which together with volcanic rocks were mined as a source for building materials until about the year 2000. The inactive quarries are still noticeable in the landscape. The urban area is bordered to the west by agricultural fields, whilst Cimatario area to the south is a natural reserve threatened by urban sprawl (Fig. 1).

The city is located north of the transition between the relatively wet and cool volcanic highlands of the Pleistocene volcanic belt and the hot and dry Chihuahua desert to the north. Eighty percent of the precipitation in Querétaro falls between May and September, as the tropical easterlies move onto the Mexican Altiplano. Rainfall totals during the winter and spring months are small to insignificant. Mean annual precipitation is low, averaging about 570 mm. Also, the region has high potential evaporation, especially in the dry season (October–April), leading to very low relative humidity throughout the year. Vegetation cover is also low; it is composed mostly of steppe shrubs, cacti, and phreatophytes. Wind intensities and directions are also strongly seasonal, with monthly mean velocities of 4 m/s throughout the year. Winds are from the E or NE about 37% of the year, and from the SW, W or NW about 25% of the time. Winter months may be affected by polar-continental air masses.

Air pollution monitoring systems were used in the city in 2005 and 2006. Fiberglass filters were installed as part of a network of monitoring stations, operated by the state university (Universidad Autónoma de Querétaro). The network is no longer operational, but

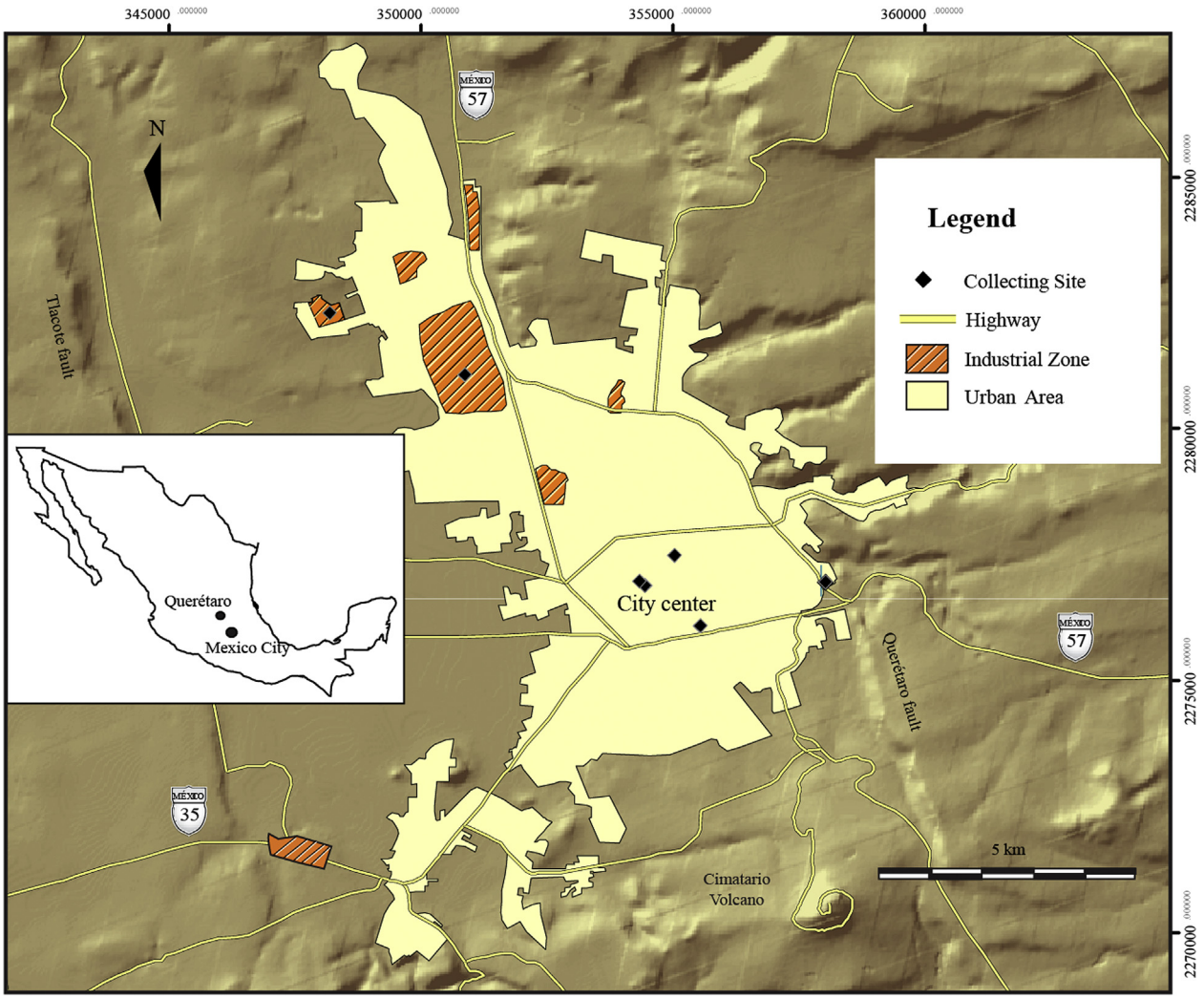

Fig. 1. Location of the stations of the manual air quality monitoring network of Querétaro city on a digital elevation model. The map also shows the distribution of industrial zones and the main roads. Fault scarps oriented almost N–S are visible and the faults indicated by their names.

the filters were stored for future use at "Centro de Estudios Académicos sobre Contaminación Ambiental" (CEACA). In 2005 the network had 7 stations distributed within the city (Fig. 1). Filters were installed on the roofs of two story buildings, two of them in areas of industrial activity and the rest around the city center. The results of the monitoring campaigns are included in the thesis work of Gasca (2007) who concluded that total suspended particle levels in the city sometimes exceeded maximum allowed levels in both the industrial zones and the downtown areas. The norm establishes a maximum of 210 $\mu g/m^3$ (Secretaría de Salud, federal norm NOM-025-SSA1-1993). Such maximum pollution levels were only surpassed during the dry season (December–March), presenting levels below code for the rainy season. Gasca (2007) suggested, based on analysis of SEM images of material extracted from filters, that most of the airborne particles are associated with industrial activities and were transported by prevailing winds to the rest of the city. The monitoring network stopped operation in 2006 due to high operation costs.

3. Materials and methods

The samples used in this study were obtained from the CEACA storage facility using non-magnetic tools. These are fiberglass air filters that were processed using the methodology described in the Mexico's federal norm NOM-035-SEMARNAT-1993, which is based on EPA standards. The filters in Hi-Vol equipment are reported to be 99% efficient in the collection of 100 μm to 0.3 μm particles. The original material was dried at room temperature (25 °C) for 24 h. It was also weighed before and after sampling. After drying, total particles were determined by gravimetric difference considering the initial weight. For the material we used, TSP was determined using an algorithm that considers the volume of air passing through the filter calculated under standard conditions corrected for temperature, atmospheric pressure, time of operation, height of the filter, and wind velocity. Meteorological data were obtained online from the state operated weather stations of the state water commission (CEA). TSP is thus reported as the concentration of particle matter per unit volume ($\mu g/m^3$). For the samples used in this study, wind velocities varied between 0 and 2.8 m/s for calmed days and 2.8 and 5.8 m/s for windy days. Some of the filters operated during rainy days (17 days), with maximum precipitation of 19.3 mm but generally less than 1 mm. There is room for uncertainly in accounting for precipitation, because rain in the city is very irregular. It may rain only in some parts of the city, precipitation events are typically of short duration, and pollution monitoring stations use weather data from the nearest CEA weather station. A day was

considered rainy if the meteorological station closest to the sampling site reported at least 3 mm of precipitation, but this does not guarantee that it rained at all TSP monitoring stations.

The material we used corresponds to samples collected weekly from 08/2005 to 12/2005 and 08/2006 to 12/2006, accounting for about two months in the rainy season and two in the dry season for each year. A total of 80 samples were divided into two groups for their analysis; this division is designed to test the whether or not contribution from vehicles or industrial activities could be isolated. Group 1 is from industrial zones, two sites in the northwest side of the city. Group 2 is from the city center including a site in the eastern side of town near a high traffic intersection.

Magnetic susceptibility measurements were obtained with an AGICO model KLY-3 Kappabridge. The bulk susceptibility was measured on 56 cm^2 of the filter area. The instruments used assume that samples are of a 10 cm^3 standard volume, whilst we used a standard area of 56 cm^2 for all samples; thus susceptibility values are relative and not absolute, but individually comparable. The diamagnetic background contribution of the sample holder was always compensated. We tested reproducibility by repeating each measurement 3 to 4 times, and averaging the results. Repeat measurements of the same sample are usually within 2% of each other. We made no attempt to correct the magnetic susceptibility for the paramagnetic contribution from the filter (fiberglass), because we determined this contribution to be relatively small ($\sim 2 \times 10^{-7}$) and similar in several clean filter samples. The frequency dependency of magnetic susceptibility was measured with an AGICO MFK1 Kappabridge at the University of Texas in Dallas, using frequencies of 0.976, 3.9 and 15.6 kHz. The X_{FD} was calculated as suggested by Hrouda (2011); we report $X_{FD(1,4)}$ and $X_{FD(1,16)}$ average values.

We determined hysteresis loops, isothermal remanent magnetization (IRM) acquisition curves, and DC backfield curves of the saturation IRM (SIRM = IRM at 1.8 T), all at room temperature. For this purpose we used a small area of the filter (9 mm^2), and we used a Princeton Measurements Corporation model Micromag 2900 vibrating sample magnetometer applying a maximum field of 1.8 T. With this we determined hysteresis parameters Ms, Mrs, Hc, and Hcr in order to estimate magnetic particle characteristics in a Day plot (Dunlop, 2002a). We modeled the different contributions to the IRM from distinct magnetic phases according to their coercivities using the method proposed by Stockhausen (1998) and developed by Kruiver et al. (2001). For the acquisition of thermomagnetic curves we used the powders extracted from 56 cm^2 of the filters. Thermomagnetic curves for selected samples were obtained in air with a home-made Curie balance, in a field of 0.4 T at cooling and heating rates of 30–40 °C min^{-1}.

Multivariate statistical analyses were performed using the R free software: R version 2.15.0 (2012). Fifty samples ($n = 26$ variables) were used for this investigation and the data set included 8 magnetic variables, 3 meteorological variables (relative humidity, atmospheric pressure and mean wind velocity), and 1 physical variable (TSP).

For scanning electron microscope (SEM) characterization of the particles, a small area of a filter was placed vertically within a beaker and particles were rinsed off using ethylic alcohol. The resulting suspension was placed in Eppendorf vials, allowing particles to sediment and dried in a furnace at 30 °C for 12 h. The particles collected were mounted on an Aluminum plate and carbon coated. Mounting was designed to avoid altering particle morphology. Finally, particles were identified using a Phillips XL30 SEM with an energy-dispersive X-ray spectrometer EDAX model DX4. Iron oxides were further identified using Raman Spectroscopy at CINVESTAV, Querétaro. The particles to be characterized by were separated with a hand magnet and mounted on a Si wafer. An individual particle was selected by an optical microscope Olympus BX40, with a 50X objective, which was coupled to a Dilor Raman spectrometer model Labram II equipped with a HeNe laser of 632.8 nm at 20 mW. A neutral density filter attenuated the laser beam power to 10 mW. We used a 2 μm spot and a diffraction grid of 1800 g/mm. All measurements were done at room temperature.

4. Results

4.1. Magnetic properties

Low field magnetic susceptibility (κ) of the filters is relatively small, ranging between about 1 and $16 \cdot 10^{-6}$ SI units. Fig. 2 shows bi-plots of magnetic susceptibility and IRM_{1T} vs. TSP under different environmental conditions and for different areas. A high positive correlation is found between susceptibility and TSP ($R = 0.928$, $P < 0.01$; Fig. 2(a)), using the total set of 82 data from 7 monitoring stations (between 6 and 24 samples per station, where a sample is one filter used for 24 h). IRM_{1T} shows a lower correlation with TSP, $R = 0.745$ (Fig. 2(b)), based on the 50 available data from IRM acquisition experiments, which were carried out for selected stations only.

For the data shown in Fig. 2, we also calculated linear regression fits for samples corresponding to rainy and no rain days. The fits are similar: the slope of rainy day data is 0.06 and for no rain days is 0.089, albeit the correlation coefficients are indistinguishable ($R \sim 0.93$). Both fits include the confidence region of the regression line of the full data set. In analyzing the subsets, however, we notice that mean TSP, k, and saturation magnetization M_s values are higher during rainy days (see Appendix). For rainy days TSP ranges between about 30 and 285 μg/m^3, whilst for no rain days they range between about 20 and 200 μg/m^3. Also, during rainy days the correlation between k and TSP decreases: from $R = 0.93$ (no rain) to $R = 0.75$ (rain), and the correlation between Ms and TSP increases from $R = 0.57$ (no rain) to $R = 0.75$ (rain). Something similar occurs when wind effects are considered, for calm days the correlation between k and TSP is $R = 0.95$ and for windy days $R = 0.86$. We further note that k and M_s are better correlated during windy days than during calm days (Appendix). We also compared the regression fits for data corresponding to the city center with those from the industrial zone and found no significant difference (Fig. 2(b)), except for IRM. TSP is better correlated with IRM for sites in the city center ($R^2 = 0.78$) than sites in the industrial area ($R^2 = 0.46$).

We calculated Pearson's coefficient and p-value for all magnetic and physical properties measured, and data are summarized in a correlation matrix (see Appendix). We observed, for instance, a statistically significant correlation ($R = 0.595$, $p < 0.01$) between TSP and hysteresis parameter Ms, but not between TSP and Mrs. The hysteresis parameter Hc correlates with TSP for windy days, but not for calm days.

Measurements dependency observed for magnetic susceptibility in a subset of 20 selected filter samples is high. $X_{FD(1,4)}$ range between about 2.1 and 12%, and between 3.2 and 9.7% for $X_{FD(1,16)}$ with an average $X_{FD(1,16)}$ of about 5.5%. We recognized the presence SP particles also by measuring the short-term temporal variation of SIRM (Worm, 1999). SIRM in a small collection of samples tested decays 4–8% in about 100 s.

Thermomagnetic curves indicate a dominant phase with a Curie temperature close to ~575 °C, the Curie temperature typical of nearly pure magnetite (Fig. 3). The curves contain additional information, but interpretation is somewhat ambiguous. Thermomagnetic curves from magnetic extracts from the industrial zone are not reversible, with reduced magnetic moments in the cooling segment of the curve indicating progressive destruction of a magnetic phase possibly through oxidation. There is a hint of a

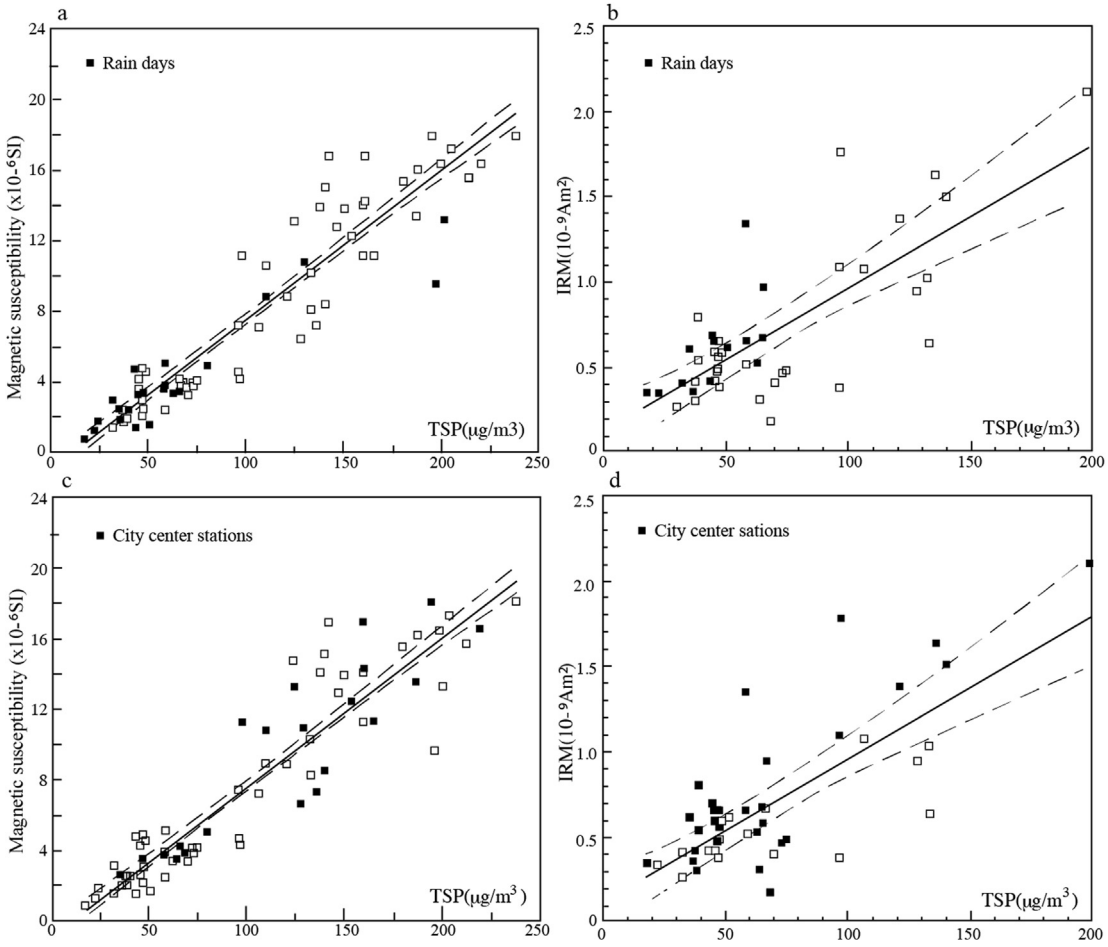

Fig. 2. (a and b) Correlation between magnetic susceptibility and TSP for the filters used in stations of Fig. 1, distinguishing data for rainy days and no rain days (a), and industrial and city center (c). The black line corresponds to the linear fit and the black dotted lines correspond to ninety-five percent of confidence. (b–d) Correlation between IRM and Total Suspended Particles for the same filters. The black line corresponds to the linear fit and the black dotted lines correspond to ninety-five percent of confidence. (b) Marks days with rain or no rain, as (d) distinguishes data for stations in the city center or the industrial zones.

magnetic phase with a Curie temperature near 270 °C, with an inflection visible in both the heating and cooling curves consistent with contributions of titanomagnetite (see Fig. 3(a)). There is also a hint of a small component with a Curie temperature of about 680 °C pointing to the presence of hematite, although the field used during the experiment (0.4 T) may not activate all hematite grains. The thermomagnetic curves are somewhat noisy due to the low mass and magnetic moment, but titanomagnetite particles were indeed observed under the SEM. Samples from the city center are also non-reversible, but more closely so than samples from the industrial

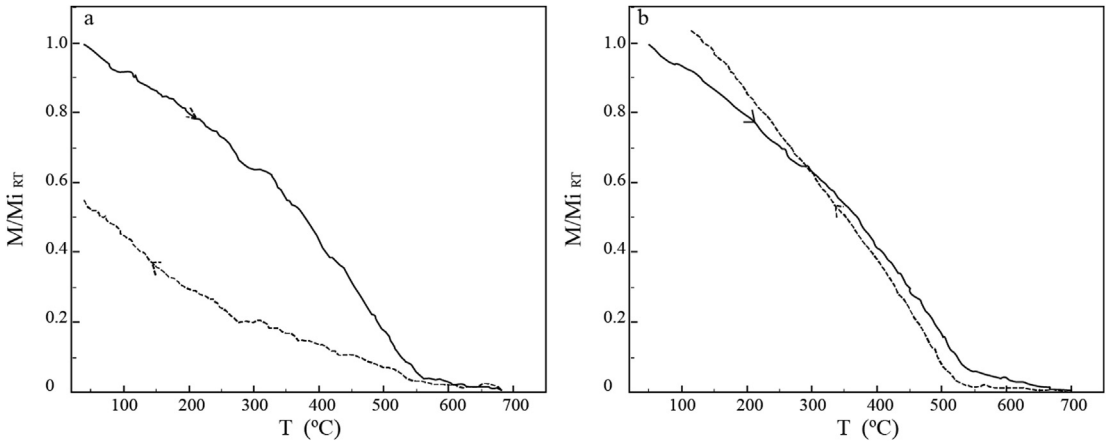

Fig. 3. Characteristic thermomagnetic curves for TSP filters, showing Curie temperatures close to that of magnetite. Units are arbitrary, M/Mi indicate the relative magnetization compared to the initial one. (a) Is a sample from the industrial zone and (b) one from the city center.

zone. The most remarkable difference observed between both areas is a slight increase in magnetic moment during cooling in the center sites, which is suggestive of maghemite which transforms to magnetite at temperatures around 350–400 °C. From Raman spectra we identified magnetite, hematite, maghemite and goethite (Fig. 4), supporting this interpretation. Based on the Curie temperatures observed, magnetite-like particles dominate the signal in the thermomagnetic curves.

Hysteresis curves for the city center (Fig. 5(a) and (b)) and industrial zones (Fig. 5(c) and (d)) are similar, being relatively narrow curves with Hc values ranging between 6 and 8 mT. These values are typical of low coercivity ferromagnetic (sensu lato) particles. There are no significant differences in the shape of the loops from central and industrial zones. Samples almost reach saturation of IRM for fields of 0.6 T (maximum applied field = 1.8 T), but a high coercivity phase is present in samples from both the city center and from an industrial park. This contribution varies at the same station during different days, not as result of seasonal variations in precipitation, but probably because of changes in wind intensity or direction. Higher hematite contributions appear to be related to prevalent westerly winds.

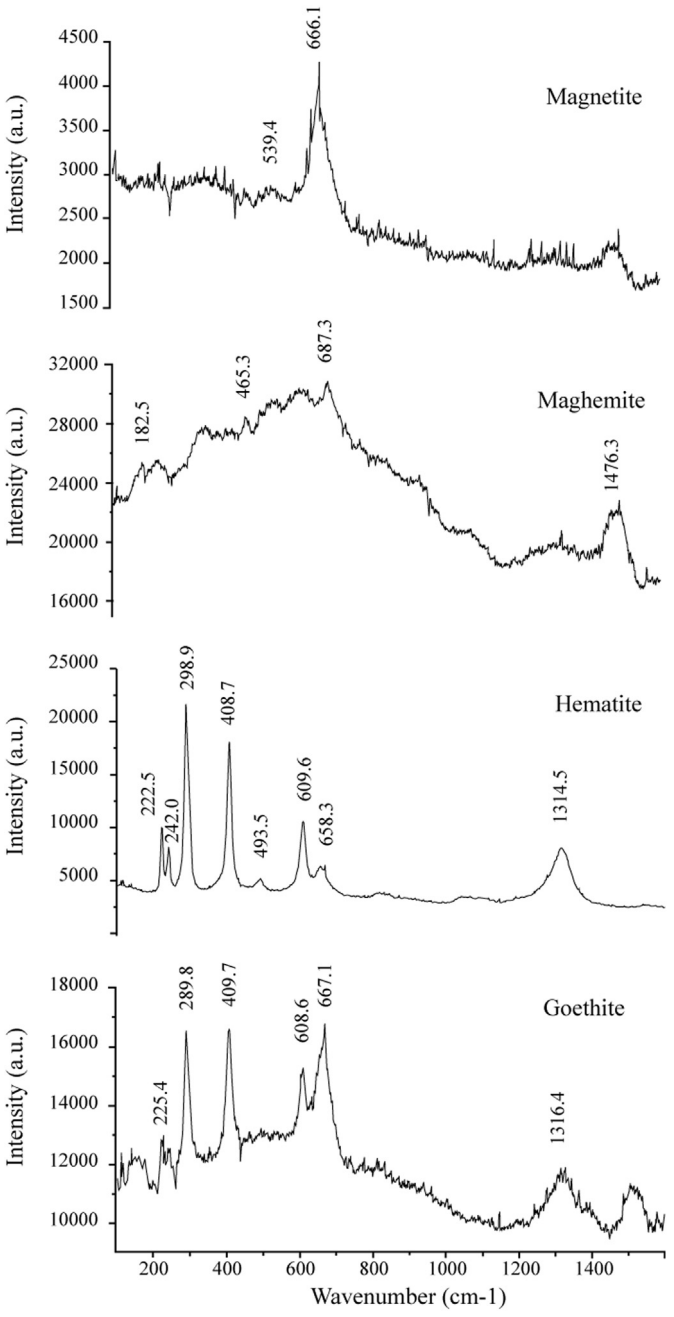

Fig. 4. Raman spectra of samples identified as magnetite, hematite, maghemite and goethite.

Hysteresis data are presented in Figs. 5 and 6. The hysteresis loops were corrected for the high-field diamagnetic and/or paramagnetic contributions of the filter matrix and other materials, and parameters are summarized in Fig. 6 on a modified (Day et al., 1977) plot. All data fall within the PSD field of the original Day plot, with a relatively wide range of Hcr/Hc values of 2.8–5.1 and a narrow Mrs/Ms variation between about 0.08 and 0.1. The data correspond the region of bimodal mixtures of populations of grains with very different sizes, and points in Fig. 6 are located to the right (in the diagram) of the linear SD + MD mixture curve of Dunlop (2002a), and correspond to the mixing curve 3 of SD + MD grains of Dunlop (2002b).

There are no evident differences between the hysteresis of powders from the city center and industrial zone. The differences between samples collected during rainy days and no rain days are also subtle; on average, rainy days show slightly higher Hcr/Hc ratios, as Hcr values are on average higher in those days (Appendix). We did not find significant differences between samples collected during windy days (days with average wind velocity >2.8 m/s) and calm days. However, that samples with the highest magnetic susceptibility values tend to occupy the region of the Day plot that can be otherwise interpreted as a mixture of multi-domain and single domain magnetite (about 80% MD). The values of k for these samples are generally greater than 8×10^{-6} SI, corresponding to sites/days with higher TSP values. The hysteresis ratios for these samples are streaked to higher Hcr/Hc than the rest of the samples, suggesting that their hysteresis curves can also be explained by a mixture of PSD particles with variable contributions of SP particles.

Various IRM acquisition curves determined for samples from both areas were modeled according to Kruiver et al. (2001), who assume a log-normal distribution of particles of different coercivity contributing to the IRM. The distribution is characterized by the values B1/2 (the field at which half of the SIRM is reached, i.e.: remanent acquisition coercivity; B1/2 is related to the coercivity Hcr, but according to Dankers (1981) is larger by a factor of about 1.5 for most minerals) and DP (the so called dispersion parameter equal to one standard deviation of the logarithmic distribution). Typical results for industrial (Fig. 7(a) and (b)) and city center (Fig. 7(c) and (d)) show subtle yet notable differences. In the city center area, the samples show a small contribution from a high coercivity phase (B1/2 > 100 mT), generally less than 10%, an occasionally no such contribution at all. The rest of the IRM can be modeled with low and moderate coercivity components, but is dominated by the moderate coercivity component with relatively narrow dispersion parameter ($B_{1/2}$ ~ 40 mT, and DP ~ 0.30). Samples from the industrial area show a larger contribution from the high coercivity component (B1/2 > 100 mT), which often reaches about 40% and is generally of higher coercivity than in the center sites. Low and moderate coercivity components in samples from the industrial zones are comparable in B1/2 and DP to samples from the city center.

4.2. Electron microscopy

We analyzed a total of 50 filter samples under the SEM with 32 samples corresponding to the city center, and 18 samples to the industrial area. A total of about 750 particles, 270 from the

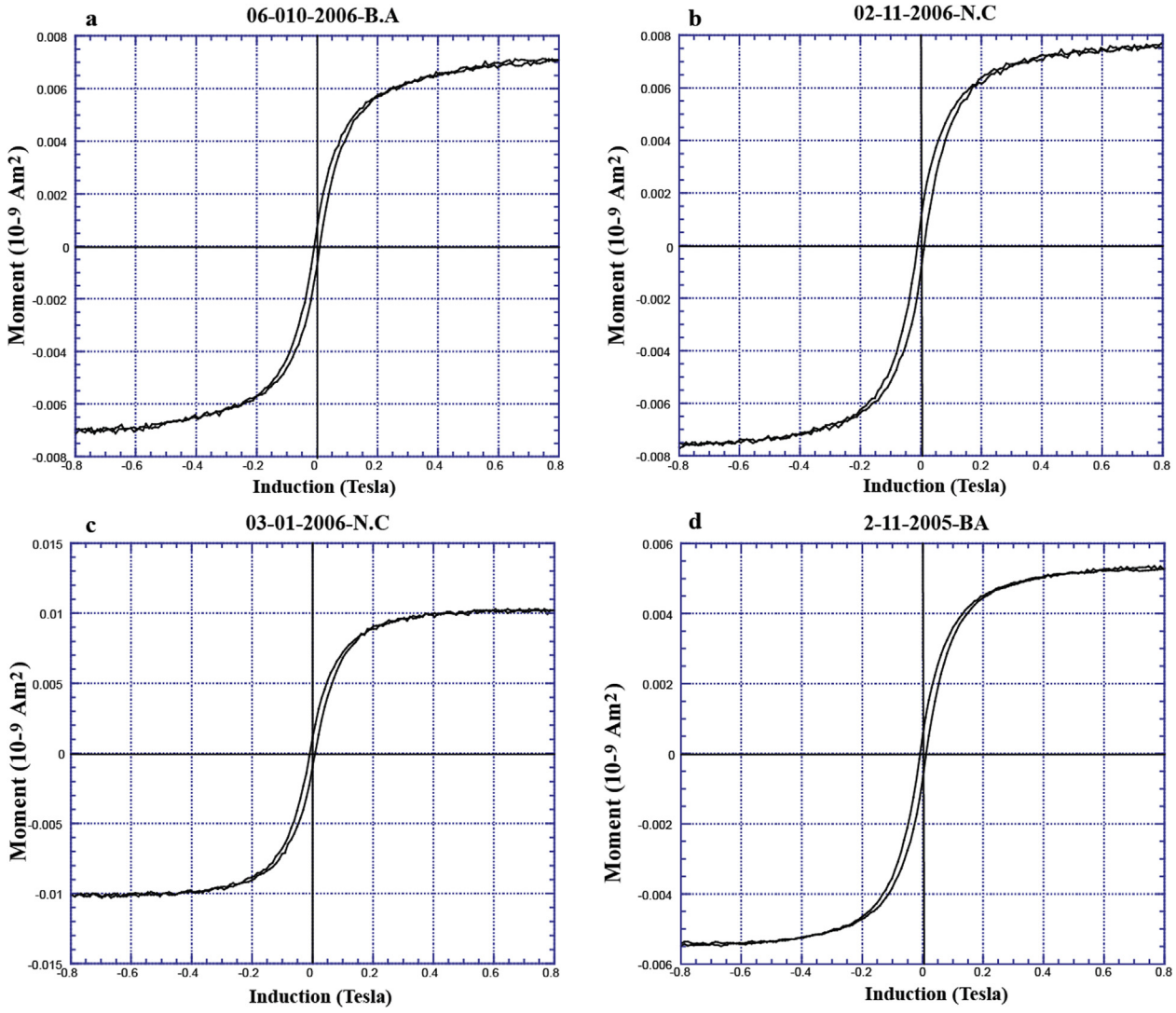

Fig. 5. Characteristic hysteresis curves corrected for the paramagnetic and diamagnetic contributions for samples from monitoring sites in the city center sites (a, b) and the industrial zone (c, d).

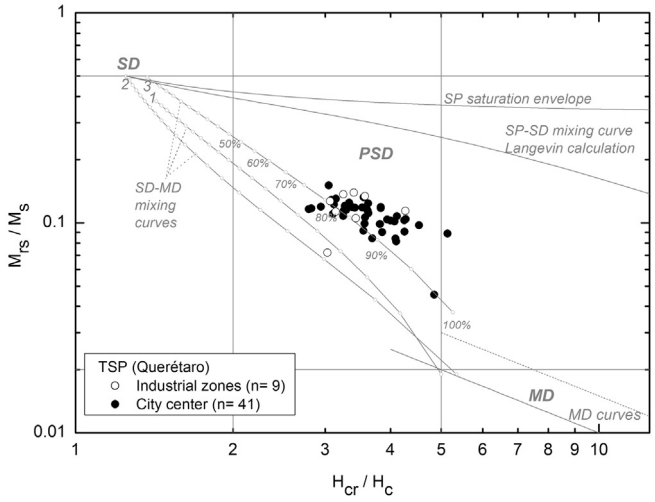

Fig. 6. Day plot (Day et al., 1977) for filter samples from the industrial area and the city center, modified after Dunlop (2002) to show theoretical mixing lines of SD + MD and SD + SP particles.

industrial area and 480 from the city center, were analyzed. Particles were classified according to their morphology and composition in natural or anthropogenic. Natural particles are generally more irregular, and their composition can be recognized as lithic material of mainly silicic composition. Metal-bearing particles are generally of anthropogenic origin, except Fe and Ti oxides, which are also common components of rocks and soils and thus may be of natural or anthropogenic origin. The provenance of such particles is therefore more difficult to decide.

Most of the anthropogenic particle populations in Querétaro are similar in both the city center and the industrial areas (Fig. 8). They have grain sizes <10 μm, and represent 74.3% of the particles for the industrial area and 60.7% for the city center (Fig. 9). Of all PM10 particles, the contribution <2.5 μm (PM2.5) is about 45% in the industrial area and ~29% in the city center. Overall, heavy metal-bearing particles are more abundant in the industrial zone except for Fe-bearing particles. Cu bearing particles are the most abundant particles in industrial areas (Fig. 8), occurring as Cu sulfides or almost pure spherical particles. They are relatively more abundant in the industrial area than in the city center. C, S, V, and Ni occur in particles generally >10 μm in both areas (Fig. 9). Particles rich in

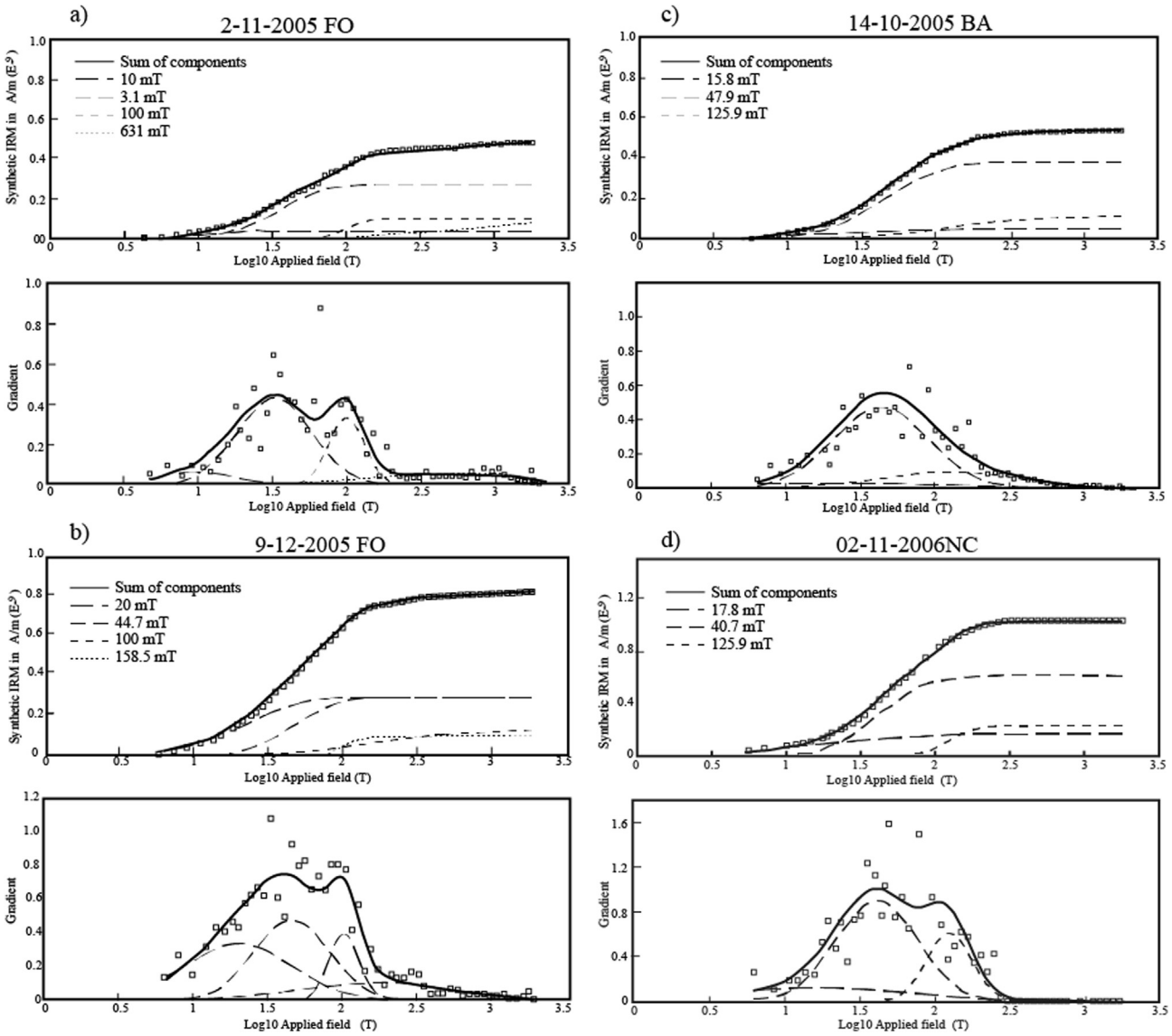

Fig. 7. IRM component analysis (Kruiver et al., 2001) for samples from the industrial park (a, b), showing the lineal acquisition curve and its gradient, and the city center (c, d). We also show the B1/2 of the modeled components to the IRM, whilst DP and the contribution from each component may be estimated in the graph.

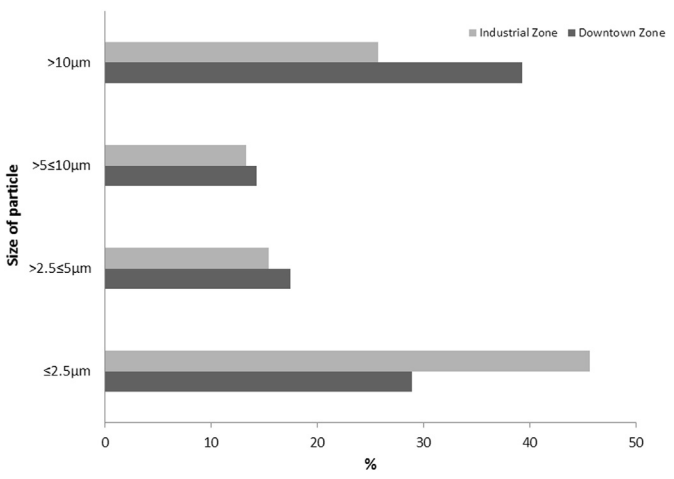

Fig. 8. Grain-size distribution (percentages) of the particles identified by SEM analysis. Notice that about 60–74% of the particles are in the range between 2.5 and 10 μm.

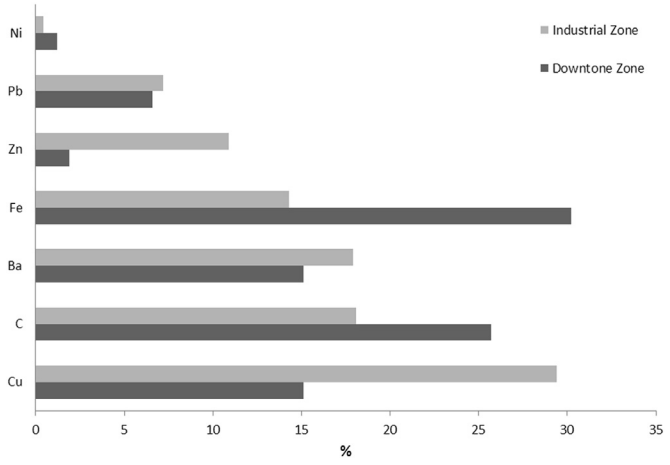

Fig. 9. Composition and percentage contribution of particles classified of anthropic origin for the industrial and city center areas of Querétaro, as identified from SEM analysis.

elemental C are more abundant in the city center area (~25%) than in the industrial area (~18%, with small grain sizes (<2.5 μm) in the latter and more variable sizes in the center area. C particles occur together with S, with traces of V and Ni, and also as almost pure C.

Ba bearing particles are common in both areas, with relative abundances of ~18% and 15% in the industrial area and the city center, respectively. We identified barite ($BaSO_4$) as well as Ba carbonate particles. Ba bearing particles are typically <2.5 μm, with the smaller sizes dominant in the center area. Although Ba may occur naturally, there are no natural Ba sources within the city or its surroundings. The particles of $BaSO_4$ have the characteristic cleavage of the mineral phase barite (Fig. 10(a)). Barite is a common component in automobile break pads (Mosleh et al., 2004), as well as Ba is used in diesel fuel as a smoke suppressant (Lim et al., 2007;

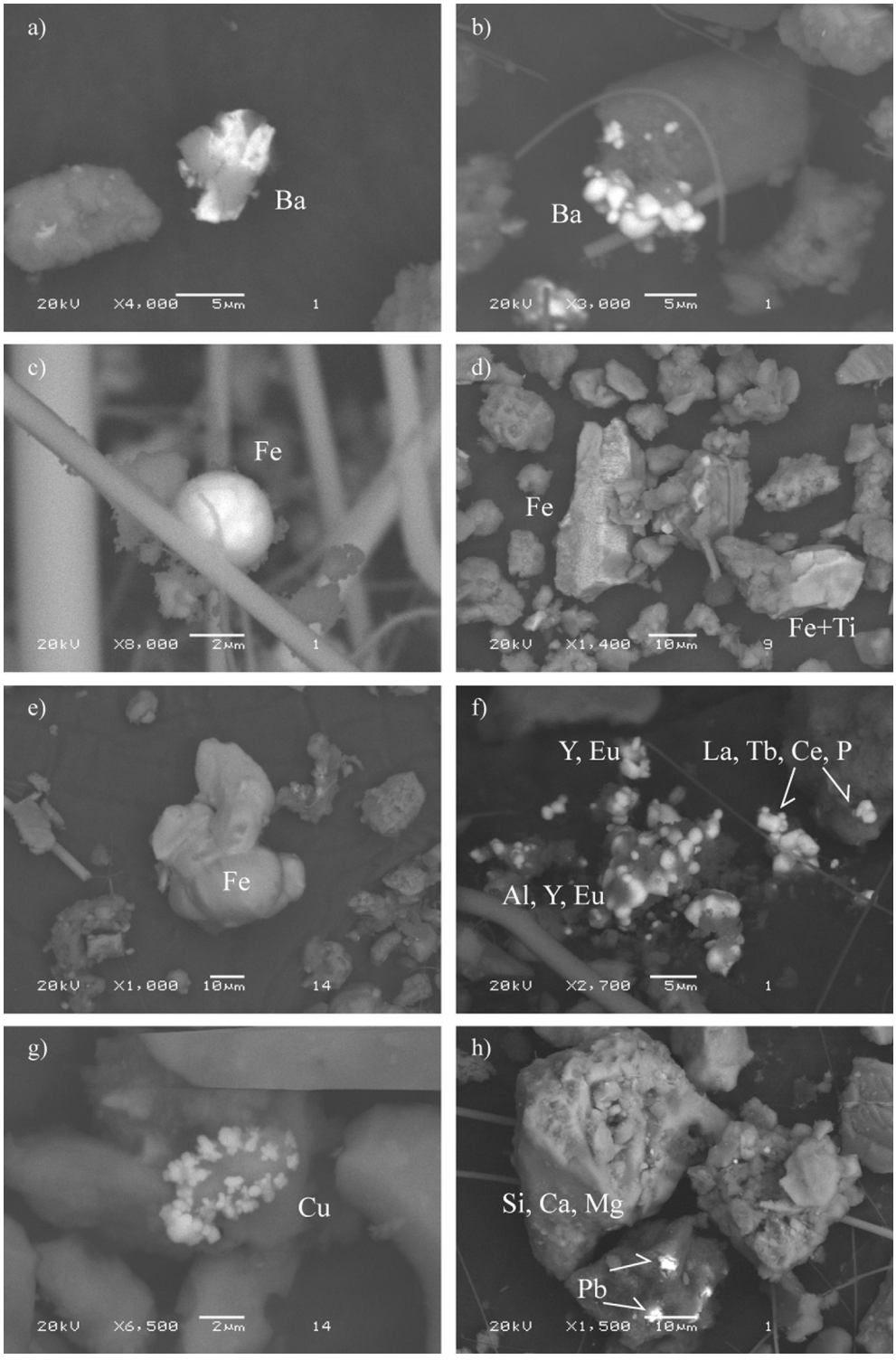

Fig. 10. Back-scattered electron SEM images of examples of the different type of particles identified in the TSP filters. See the text for additional explanation.

Maher et al., 2008); this is thus the most likely source. In other cities it has been also associated with glass manufacturing and pigment elaboration. A smaller population of semi-spherical $BaSO_4$ particles was also identified.

Fe-bearing particles identified represent 14.3% and 30.2% of the relative abundance in the industrial and city center zones, respectively. We observed spherical Fe–O particles, occasionally associated with Cr and Ni, alloys with Zn, irregular shaped Fe–O particles, and irregular Fe–O particles associated with Cr–Ni. Fe-rich particles of grain-size <2.5 μm show higher relative abundance in the city center than in the industrial zones (Fig. 8).

Zn and Pb-bearing particles are also commonevident, representing 10.9% of the particles of anthropic origin in the industrial area and about 5% in the city center. Zn occurs as rounded, acicular, and spherical Zn–O particles; most of them are <2.5 μm (Fig. 9) with this small particle size more common in the city center. Pb-bearing particles represent 7.2% and 6.6% of the total particles analyzed in the industrial and center zones, respectively. Pb occurs as sulfide and occasionally as irregularly shaped oxide. A minor population of Pb particles corresponds to spherical Pb–S–O particles and Pb–Cu–Fe particles. Irregularly shaped Pb-bearing particles may be associated with S–O, S, Sn, Sb, Cu, Cr, and Fe. These particles as well are predominantly <2.5 μm, in both zones.

Other less abundant particles include the elements Ni, Cd, V, Sn, Ce, Mo, W, Zr, Ca, As, Sb, Mn, Hg, Bi, Ti, Sr, Se and Cr, and rare earths. Ni rich particles are 0.45% and 1.2% in the industrial and center zones, respectively. Spherical Ni particles are associated with Fe and V. Minor populations include spherical to irregular particles of metallic Ni and Ni–Cu associations. They are present in both areas as particles generally <5 μm. The rest of the metallic particles represent a percentage of less than 1% of the total in both zones. Metal-bearing particles restricted to the industrial zone include Mn, Hg, Bi, Ti, Sr, Se y Cr, whilst Cd and Mo particles are restricted to the city center.

In summary, the great majority of the airborne particles identified in the monitoring sites in the industrial zone are also present in the city center sites. Examples of the particles identified are illustrated in Fig. 10, where we show images of the most common particles and their characteristic shape and size. We also emphasize elements that have been identified as toxic, of either natural or anthropic origin.

Iron oxide particles of spheroidal shape (Fig. 10(c)) such as those identified in this study have been also recognized in San Luis Potosí. These particles have been linked to smelting, such as in the elaboration of bronze, aluminum and steel. Spherical particles are also a by-product of welding (Aragón et al., 2000). We identified Fe–Ti oxides (Fig. 10(d)), which based on their morphology are interpreted as the natural phases titanomagnetite and ilmenite (abundant components of volcanic rocks such as basalts). Other Fe-oxide particles have irregular shape and are associated with the presence of Cr and Ni, suggesting an anthropic source. They are generally associated with wear and corrosion of metallic structures exposed to the environment (Aragón et al., 2000), as well as wear of some automobile-parts (Schauer et al., 2006). The monitoring sites in the city center show greater abundance of these particles, suggesting they are mostly produced by vehicle wear – either heavy trucks or public transport vehicles (Marié et al., 2010).

Fig. 10(f) shows the presence of rare earth elements, such as Eu, La, Y, and Tb. These elements are a component of the catalytic converters of cars and occur in the filters as particles generally smaller than 3 μm. Cu rich particles represent the most abundant particles in the monitoring sites of in the industrial zones, where they occur as dendritic particles (Fig. 10(g)) suggested to be of anthropic origin. We recognized Pb–S compounds, as particles of about 2 μm in size (Fig. 10(h)) and typically of irregular shape, assigned to be of anthropic origin.

5. Discussion

The magnetic susceptibility measurements of the filters show a good a linear correlation with the independently determined concentrations of total suspended particles. A positive correlation indicates that higher TSP values correspond to high magnetic susceptibilities. The correlation coefficient calculated for the entire data set is 0.928 and it is statistically significant, which suggests that the magnetic susceptibility is well related with the concentration of the powders collected in the filters used for monitoring atmospheric pollution in the city of Querétaro. The highest values for the magnetic susceptibility were observed in the town center, but good linear correlations were observed in both industrial and city center sites. This suggests that magnetic susceptibility values can be used as a proxy for atmospheric pollution in Querétaro. The higher abundance of Fe particles in the city center and the higher k values observed there suggest that vehicle emissions are an important source of pollution, in contrast to what was previously reported by (Gasca, 2007) for this city and supporting previous claims by INEGI (2003).

The results from magnetic measurements about mineralogy, such as the Curie temperature and IRM acquisition and modeling, show that the dominant magnetic carrier of the sampled atmospheric dust is magnetite with particles of low and moderate coercivity, with a variable and at times significant contribution from hematite, and perhaps minor maghemite as suggested by thermomagnetic curves. Raman spectroscopy, as well as magnetic measurements, confirm that magnetite, hematite, maghemite and goethite are present. In IRM acquisition curve modeling there are populations with $B_{1/2}$ of about 15 and 45 mT, representing magnetite and maghemite, around 100 mT representing hematite, and minor component of about 450 mT possibly representing goethite.

Hysteresis curves and the Day plot are consistent with a distribution of magnetic particles grain-size in a relatively narrow range of PSD sizes, but equally well explained as a mixture of SD + MD grains with a variable contribution from SP particles. The plot should be interpreted with caution, because of the presence of hematite, which tends to increase Hcr values. The overall similarity of this observation with the distribution of loess samples in a Day plot may suggest a contribution from SP particles. The hysteresis data are similar to some ceramic materials and Chinese loess, which are offset towards the SD + SP region with respect to SD–MD mixtures to the region of higher coercivity ratios. Our hysteresis results seem comparable with those in Sagnotti et al. (2009), for example, although magnetic particle matter reported in Rome in that study appears to have higher contributions from SD and SP particles. The result obtained is contrary to what was observed by Górka-Kostrubiec et al. (2012); these authors report higher Hcr/Hc and Mrs/Ms values for low susceptibilities.

The statistically significant correlation observed between TSP and hysteresis parameter Ms, but not between TSP and Mrs, may indicate a contribution from paramagnetic or SP particles to the magnetic signal. All magnetic materials contribute to Ms, but only ferromagnetic particles contribute to Mrs. This conclusion is supported by frequency dependence of susceptibility (Dearing et al., 1996). The relaxation times of the order of 10^2 s observed in IRM are suggestive of particles near the SD-SP threshold. Frequency dependence values averaging about 5.5% in turn suggest contributions to the susceptibility greater than about 10% of SP particles (Dearing et al., 1996).

The effects of climate in the relationship between magnetic parameters and TSP are small, but noticeable. In particular we found a better correlation between k and TSP on calm days and days with no rain. We also observed that, on average, suspended particle

matter (PM) decreases during rainy days. On average too, dry days after rainy days show high values of suspended PM that we attribute to greater evaporation capacity and subsequent agglomeration of very fine particles. As expected, fine particles are removed from the atmosphere by precipitation. During rainy days the correlation between k and TSP decreases, whilst the correlation between Ms and TSP increases. Something similar occurs for calm days. It thus appears that in dry calm days the concentration of PM and susceptibility increase, which may be explained by contributions from SP particles. During rainy days those particles are removed from the atmosphere and not re-suspended. The improved correlation between Ms and k during windy days is attributed to a higher capacity for mixing particles of all magnetic types in the atmosphere.

SEM results (Fig. 10) show that there are significant differences between the type of particle found in industrial and downtown areas. For instance, small particles are more abundant in the industrial area where Cu is the most common metal. There are, thus, some similarities in the particle types and particle sizes, which partially support the claim that a part of the particles in the downtown area may arise from the industrial area, but the magnetic assemblage of particles of both areas appears to be different. It is possible that industrial derived particles are present in different areas of the city. As visible in Fig. 1, the industrial areas are close to the downtown, and the emitted PM can be easily dispersed in a range of a couple of kilometers (Bidegain et al., 2011).

There is a significant proportion of particles of anthropogenic origin as suggested by Gasca (2007), but natural materials (mostly silicates but including Fe–Ti oxides) are also present. The particles of higher coercivity may be interpreted as hematite and goethite of natural and anthropic origin; they are apparently more abundant in the industrial areas with respect to the city center, but the TSP values are not necessarily greater. When the number of silicate particles identified are compared with the total, their proportion suggest that natural Fe oxides (that make a small percentage of the volume of intermediate-mafic volcanic rocks) make only a small percentage of the oxides observed. A Fe-smelting plant in the industrial area west of downtown may be a source of magnetite/maghemite and hematite, which have been observed in fly ash (Blaha et al., 2008; Jordanova et al., 2003). Hematite is evident in the IRM data, but it may not be fully represented in thermomagnetic curves due to its low magnetic moment, the field used in the magnetic balance, and inefficiency in the separation of hematite particles during sample preparation. Such particles contribute to the TSP estimate, but weakly to the IRM and to the susceptibility signal. We suggest that hematite is present in both areas, but that in the city center its signal is overwhelmed by anthropic magnetite. The IRM acquisition curves show only modest increase in magnetization between 1 and 1.8 T, generally less than 3%, we thus do not believe that hematite alone explains the poor correlation between TSP and IRM_{1T}. We infer that contributions from SP and paramagnetic particles explain why magnetic susceptibility correlates better than IRM with TSP. The worse correlation between TSP and IRM observed in the city center, compared to industrial areas, suggest that SP particles are more abundant in the downtown monitoring sites. The poor correlation between PM and SIRM or Mrs, but good correlation between PM and Ms, suggest that the paramagnetic fraction also contributes to the pollution signal. This is also supported by important paramagnetic contributions to the hysteresis curves.

We also note that highest pollution levels (TSP values) are seen in the downtown area, which has higher vehicle traffic than the industrial zone. In summary, this suggests that the pollution in both areas is derived from industrial and vehicle sources, with a higher contribution from vehicles in the downtown area. The observation of a modest correlation between IRM and TSP for the industrial area, but no correlation for the city center is to be expected because of the different magnetic structure of the particle assemblages. In Fig. 6 we show the dominant domain type for the assemblage of magnetic particles collected in the filters. In general, it is possible to observe that the prevalent magnetic fraction is in the pseudo-single domain range, both for industrial and downtown samples, which could also result from a mixture of SD, MD, and SP particles. The presence of particles in the PSD range is supported by the SEM observations, as in both areas most of the particles are about 10 μm or less in size. About 74% of the particles in the industrial sites and about 60% in the city center sites fall in that category (Fig. 10). Large particles (>20 μm) in the MD range were not observed. Of the total of less than 10 μm particles about 45% and about 30% correspond to particles of less than 2.5 μm, for the industrial and city center sites respectively. This supports, as it does the Day plot (Fig. 6), that magnetite has a grain-size in the SD to PSD range, with contributions from SP particles. Again, The presence of SP particles is indicated by room temperature decay of the SIRM in laboratory timescales and by frequency dependency of magnetic susceptibility. Both Mrs/Ms and Hcr/Hc ratios are indicative of particles whose grain-size is between about 1 and 10 μm (Day et al., 1977). This particle grain-size range is also consistent with the modeled coercivities for magnetite in IRM acquisition curves, for which coercivities (H1/2) are of a similar value.

From the combination of rock magnetic data and SEM observations we can also conclude that these magnetic particles are not part of larger minerals such as lithics or other complex compounds. This is important because this type of particles are of particular health concern, since this particle grain-size is similar in size and density to heavy metals that can be inhaled to reach the lungs.

It is also clear from SEM observations that the magnetic susceptibility signal is a combination of natural and anthropogenic Fe oxides, anthropic particles being dominant. We infer that arid conditions and lack of vegetation cover may explain the presence of natural Fe oxides, such as hematite and magnetite. Our SEM observations confirm that mineral dust is an important component of the TSP. Most common mineral dust particles are silicates (Fig. 10(h)), but calcite, magnetite, ilmenite, hematite and clay minerals are also present. Because we lack quantitative chemical analyses of the TSP we cannot determine directly if magnetic concentration parameters are a good proxy for non-ferrous heavy metal such as Pb, Cu, Sb, Zn, etc.

We found a good correlation between TSP and magnetic susceptibility. The empirical relation is dependent on the local environmental conditions as concluded by Sagnotti et al. (2006). The fact that there is a significantly better correlation between susceptibility and TSP than between SIRM and TSP indicates that susceptibility is a better proxy than other magnetic concentration parameters.

6. Conclusions

Our study of Hi-Vol filters used for air quality monitoring in the city of Querétaro shows that magnetic susceptibility is a good approximation of low-level atmospheric dust, and would allow easy spotting of critical areas in terms of pollution levels. The good correlation observed between magnetic susceptibility and the traditional method to determine TSP suggests that magnetic susceptibility is a low-cost, rapid, and efficient tool for future monitoring of air quality. Our results suggest also that magnetic susceptibility is a more effective indicator of pollution than IRM because of contributions from SP particles. According to thermomagnetic curves, IRM acquisition curves and hysteresis loops the main magnetic carrier throughout the city is low-Ti magnetite but hematite contributions are also important, with subtle distinctions

between monitoring sites in the city center and industrial areas. Hematite may contribute as much as 40% to the IRM of PM collected in the industrial areas, but that contribution is generally smaller; naturally this implies that hematite concentration by volume is locally higher than magnetite. Raman spectroscopy recognized the presence of magnetite, hematite, maghemite and goethite. Magnetite morphology and its distribution in the city suggest that it is mostly derived from vehicular sources, such as breaking system ware and combustion engines and other vehicular processes.

Magnetite has a grain-size in the SD to PSD range, with contributions from SP particles. Natural (titano) magnetite, hematite and goethite, however, are also present. SEM analyses show the presence of particles with distinct morphologies and grain-size. From EDS spectra we identified the presence of Fe oxides, as well as toxic metals. Magnetite was found as irregular shape aggregates as well as semi-spherical particles. The aggregates are commonly associated with other heavy metals.

As in Shanghai city (Shu et al., 2001) we observed high and low coercivity phases, but not in similar proportions. Even though magnetite dominates the magnetic signal, IRM data suggests that particles of hematite may be much more abundant by weight. We also found that the high-coercivity phase contribution is variable within a station, and within a season. This variability is interpreted to reflect wind intensity, and variable contributions from distal sources. This hypothesis requires further testing. The contributions from SP particles were observed in mid-latitude cities as well. We do not find, however, a significant difference between winter and summer months. Our sites in arid central Mexico do record a strong dependence of concentration parameters on precipitation, as reported by Muxworthy et al. (2001). Frequency dependence values observed in the central Mexico sites appear relatively high compared to studies in central Europe and Asia.

Acknowledgments

We thank Marina Vega González for her help in the SEM and Antonio Aranda Regalado and the CEACA at Universidad Autónoma de Querétaro for allowing access to the filters of the RMMA. We thank also Jorge Escalante for his help in construction and operation of the Curie balance. This research was partly supported by Posgrado en Ciencias de la Tierra, UNAM. We thank Francisco Rodríguez Melgarejo from CINVESTAV for helping with Raman spectroscopy. We also thank two anonymous reviews for their comments, which greatly improved this contribution.

Appendix A. Supplementary data

Supplementary data related to this article can be found at http://dx.doi.org/10.1016/j.atmosenv.2014.07.015.

References

Aragón, A., Torres, G., Monroy, M., Luszczewski, A., Leyva, R., 2000. Scanning electron microscopy and statistical analysis of suspended heavy metal particles in San Luis Potosi, Mexico. Atmos. Environ. 34, 4103–4112.

Bidegain, J.C., Chaparro, M.A.E., Marié, D.C., Jurado, S., 2011. Air pollution caused by manufacturing coal from petroleum coke in Argentina. Environ. Earth Sci. 62 (4), 847–855.

Blaha, U., Sapkota, B., Appel, E., Stanjek, H., Rösler, W., 2008. Micro-scale grain-size analysis and magnetic properties of coal-fired power plant fly ash and its relevance for environmental magnetic pollution studies. Atmos. Environ. 42, 8359–8370.

Böhm, P., Wolterbeek, H., Verburg, T., Mulisek, L., 1998. The use of tree bark for environmental pollution monitoring in the Czech Republic. Environ. Pollut. 102, 243–250.

Dankers, P., 1981. Relationship between median destructive and remanent coercive forces for dispersed natural magnetite, titanomagnetite and hematite. Geophys. J. Int. 64, 447–461.

Day, R., Fuller, M., Schmidt, V.A., 1977. Hysteresis properties of titanomagnetites: grain size and compositional dependence. Phys. Earth Planet. Inter. 13, 260–267.

Dearing, J.A., Dann, R.J.L., Hay, K., Lees, J.A., Loveland, P.J., Maher, B.A., O'Grady, K., 1996. Frequency-dependent susceptibility measurements of environmental materials. Geophys. J. Int. 124, 228–240.

Dunlop, D.J., 2002a. Theory and application of the Day plot (Mrs/Ms versus Hcr/Hc) 1. Theoretical curves and tests using titanomagnetite data. J. Geophys. Res. 107 http://dx.doi.org/10.1029/2001JB000486.

Dunlop, D.J., 2002b. Theory and application of the Day plot (Mrs/Ms versus Hcr/Hc). 2. Application to data for rocks, sediments, and soils. J. Geophys. Res. 107 (B3), 2057. http://dx.doi.org/10.1029/2001JB000487.

Evans, M.E., Heller, F., 2003. Environmental Magnetism: Principles and Applications of Enviromagnetics. In: International Geophysics Series, vol. 86. Academic Press.

Gasca, M., 2007. Caracterización por SEMEDS de aeropartículas antrópicas de la fracción respirable en la Ciudad de Querétaro y su relación con fuentes contaminantes (Thesis). Universidad Autónoma de Qurétaro, p. 154.

Górka-Kostrubiec, B., Król, E., Jeleńska, M., 2012. Dependence of air pollution on meteorological conditions based on magnetic susceptibility measurements: a case study from Warsaw. Stud. Geophys. Geod. 56, 861–877. http://dx.doi.org/10.1007/s11200-010-9094-x.

Hrouda, F., 2011. Models of frequency susceptibility of rocks soils revisited and broadened. Geophys. J. Int. 187, 1259–1269.

Instituto Nacional de Estadística Geográfica e informática INEGI, 2003. Anuario Estadístico Querétaro de Arteaga.

Instituto Nacional de Estadística Geográfica e informática INEGI, 2010. Censo Nacional de Población y Vivienda.

Jordanova, N.V., Jordanova, D.V., Veneva, L., Yorova, K., Petrovsky, E., 2003. Magnetic response of soils and vegetation to heavy metal pollution—a case study. Environ. Sci. Technol. 37, 4417–4424.

Kruiver, P.P., Dekkers, M.J., Heslop, D., 2001. Quantification of magnetic coercivity components by the analysis of acquisition curves of isothermal remanent magnetisation. Earth Planet. Sci. Lett. 179, 205–217.

Lim, M.C.H., Ayodo, G.A., Morawska, L., Ristovski, Z.D., Jayaratne, E.R., 2007. The effects of fuel characteristics and engine operating conditions on the elemental composition of emissions from duty diesel buses. Fuel 86, 1831–1839.

Maher, B.A., Moore, C., Matzka, J., 2008. Spatial variation in vehicle-derived metal pollution identified by magnetic and elemental analysis of roadside tree leaves. Atmos. Environ. 42, 364–373.

Marié, D.C., Chaparro, M.A.E., Gogorza, C.S.G., Navas, A., Sinito, A.M., 2010. Vehicle-derived emissions and pollution on the road Autovia 2 investigated by rock-magnetic parameters: a case of study from Argentina. Stud. Geophys. Geo. 54 (1), 135–152.

Moreno, E., Sagnotti, L., Dinarès-Turell, J., Winkler, A., Cascella, C., 2003. Biomonitoring of traffic air pollution in Rome using magnetic properties of tree leaves. Atmos. Environ. 45, 2967–2977.

Mosleh, M., Blau, P.J., Dumitrescu, D., 2004. Characteristics and morphology of wear particles from laboratory testing of disk brake materials. Wear 256, 1128–1134.

Muxworthy, A., Matzka, J., Petersen, N., 2001. Comparison of magnetic parameters of urban atmospheric particulate matter with pollution and meteorological data. Atmos. Environ. 35, 4379–4386.

Sagnotti, L., Macri, P., Egli, R., Mondino, M., 2006. Magnetic properties of atmospheric particulate matter from automatic air sampler stations in Latinum (Italy): toward a definition of magnetic fingerprints for natural and anthropogenic PM10 sources. J. Geophys. Res. 111, B12S22. http://dx.doi.org/10.1029/2006JB004508.

Sagnotti, L., Taddeucci, J., Winkler, A., Cavallo, A., 2009. Compositional, morphological, and hysteresis characterization of magnetic airborne particulate matter in Rome, Italy. Geochem. Geophys. Geosyst. 10, Q08Z06. http://dx.doi.org/10.1029/2009GC002563.

Schauer, J.J., Lough, G.C., Shafer, M.M., Christensen, W.F., Arndt, M.F., DeMinter, J.T., Park, J.S., 2006. Characterization of metals emitted from motor vehicles. Health Eff. Inst. Res. Rep. Health Eff. Inst. 133, 1–76.

Shu, J., Dearing, J.A., Morse, A.P., Yu, L., Yuan, N., 2001. Determining the sources of atmospheric particles in Shanghai, China, from magnetic and geochemical properties. Atmos. Environ. 35, 2615–2625.

Stockhausen, H., 1998. Some new aspects for the modeling of isothermal remanent magnetization acquisition curves by cumulative log Gaussian function. Geophys. Res. Lett. 25 (12), 2217–2220.

Voutsa, D., Samara, C., 2002. Labile and bioaccessible fractions of heavy metals in the airborne particulate matter from urban and industrial areas. Atmos. Environ. 36, 3583–3590.

Worm, H.U., 1999. Time-dependent IRM: a new technique for magnetic granulometry. Geophys. Res. Lett. 26 (16), 2557, 1999GL008360.

Xie, S., Dearing, J.A., Boyle, J.F., Bloemendal, J., Morse, A.P., 2001. Association between magnetic properties and element concentrations of Liverpool street dust and its implications. J. Appl. Geophys. 48, 83–92.